Anodic titanium oxide: A new template for the synthesis of larger diameter multi-walled carbon nanotubes

I. Eswaramoorthi, Lian-Pin Hwang *

Institute of Atomic and Molecular Sciences, Academia Sinica and Department of Chemistry, National Taiwan University, Taipei 106, Taiwan

Abstract

Carbon nanotubes (CNTs) with larger diameter were synthesized over anodic titanium oxide (ATO) template by CVD method using acetylene as carbon source. The porous titanium oxide was obtained by anodization of titanium metal in a mixture of 1 M H_2SO_4 + 0.5% HF electrolyte at a constant applied potential of 40 V. The XRD analysis of anodized titanium revealed that rutile and anatase forms of TiO_2 are formed due to anodization. Further, SEM analysis was used to follow the development of pores on titanium surface. The TEM analysis revealed that the formed CNTs are straight and hollow with uniform wall thickness as well as larger diameter (70–80 nm). HRTEM study showed that the formed CNTs are multi-walled and their wall thickness is around 2–3 nm. Further, the structural features of the formed CNTs were studied by XRD. Raman spectroscopy was used to study the degree of graphitization of CNTs. The Lewis acid sites of TiO_2 present in the internal surface of the pores play an important role in the catalytic decomposition of acetylene and hence the formation of CNTs. When increasing the carbon deposition time, the wall thickness of CNTs is not increased significantly, indicating that the decomposition of acetylene is due to Lewis acid sites of TiO_2 and not due to thermal decomposition. Further, the morphology of CNTs formed over ATO template was compared with that of CNTs formed on Co electrodeposited ATO. There is no significant difference in morphology as well as wall thickness was observed between the CNTs grown over ATO with and without Co catalyst. But, still further investigations are necessary to study the structural differences between the CNTs grown over ATO with and without Co catalyst.
© 2007 Elsevier B.V. All rights reserved.

Keywords: Nanotubes; Chemical vapor deposition; Morphology; Nanotechnology

1. Introduction

Carbon nanotubes (CNTs) are tubular sp^2-like carbons with nanoscale dimensions that exhibit fascinating electrical, mechanical, thermal and optical properties which make them very promising in various potential applications [1–9]. Extensive efforts have been made to control the growth and properties of CNTs. Different growth techniques including arc discharge [10], plasma techniques [11,12], laser ablation [13] and pyrolysis of hydrocarbon vapor over various catalysts [14] have been used to control the position, direction and arrays of CNTs. Recently, growth of CNTs over porous template such as anodic aluminum oxide (AAO) inspired a new way to grow well ordered CNTs with uniform size and shape due to the well ordered pore structure with narrow size distribution and uniform inter-pore spacing [15,16]. The AAO template with various pore size and distribution patterns can be easily obtained by varying the oxidation voltage and the acid electrolyte and hence electrochemically prepared porous alumina is considered as one of the most important template material. Highly ordered graphite nanofibers were formed by pyrolysis of ethylene followed by annealing at a temperature less than 600°C over Ni-catalyst activated AAO [17]. Ultrafine carbon tubes were formed in AAO without catalyst by pyrolytic carbon deposition from propylene at 800 °C [18]. The obtained CNTs showed low crystallinity, but with certain atomic plane orientation in the carbon tubes. Electrochemically deposited cobalt particles in the pore bottom of the AAO template resulted in the formation of CNTs by acetylene pyrolyzing at 650 °C [15]. The proposed mechanisms were that cobalt particles might promote the

decomposition or initiate the tube growth through the initial catalytic decomposition [19]. Naturally, the question arises whether other value metals such as Ti, Ta, Nb, V, Hf and W can also be used to grow the CNTs inside the pore arrays fabricated by the anodization process, similar to AAO. The surface of these value metals is usually covered with a native oxide film of a few nanometers when these metals are exposed to oxygen containing surrounding. Current state-of-the-art techniques for aluminum anodization using self-assembly of pores allow the fabrication of monodomain and monodisperse porous alumina structures with adjustable pore size and depth. Generally, the formation of highly ordered pores is based on lithographic definition of etch initiation sites or be completely due to self-organization. However, porous templates based on other value metals by the anodization process have been rarely studied. Among the value metal oxides, titanium dioxide is considered as a promising material for photocatalysis, catalyst support and implants [20,21]. Zwilling et al. [22,23] reported that a porous TiO$_2$ layer is created by anodization in a chromic acid solution in the presence of a small amount of HF, whereas only the barrier TiO$_2$ layer is formed in pure chromic acid contrary to porous alumina. The compact films grown in chromic acid solution are amorphous and the porous films grown in the chromic acid–HF solution are partially crystalline. The growth mechanism in fluorinated electrolyte involves a competition between dissolution and oxide formation, in which the Cr^{VI} ions and fluorine species play locally a respective poisoning and antidote role, resulting in the growth of porous film. Further they reported that the thickness of TiO$_2$ barrier oxide is independent of anodization time, whereas that of the porous oxide of titanium increases with anodizing time as well as applied voltage. Gong et al. [24] studied the anodic oxidation of Ti in aqueous solution containing 0.5 to 3.5 wt.% HF. The obtained tubes are well aligned and organized into high-density uniform arrays with barrier layer at their bottom. The tube diameter (25–65 nm) was found to increase with anodizing voltage. Further they claimed that the final thickness (or length of TiO$_2$ tubes) of porous TiO$_2$ structure formed in diluted HF solution is independent of the anodizing time. Recently, Beranek et al. [25] produced highly ordered porous TiO$_2$ in H$_2$SO$_4$ electrolyte containing 0.15 wt.% HF. However, the thickness of the pores is still limited up to 500 nm. Also, Choi et al. [26] compared the anodization of nanoimprinted titanium with porous alumina and found that the anodized titanium films have more complicated morphologies than anodized alumina. Due to the semiconducting properties of TiO$_2$, a mirror image of the behavior of porous alumina can not be accomplished. Since, TiO$_2$ is widely used as catalyst, photocatalyst and catalyst support in a number of chemical transformations, the porous TiO$_2$ obtained by the anodization process can also be used as a template as well as a catalytic material for the growth of CNTs. The possibility to prepare ordered porous TiO$_2$ by anodization and their Lewis acid sites are considered as important features to grow CNTs. Up to now no report is available on the usage of anodized TiO$_2$ as template for CNTs growth. Hence, in the present study, we aimed to grow the CNTs over anodized TiO$_2$ by CVD method and to study their morphology and structural

features using various instrumental techniques and to compare the morphology of CNTs grown with and without Co catalyst over porous TiO$_2$ template.

2. Experimental

2.1. Anodization of titanium

A piece of commercially pure titanium metal (Giedmann, 99.5% purity) was washed with acetone and distilled water and dried in N$_2$ atmosphere. The native oxide already formed on Ti metal surface was removed by chemical treatment with a mixture of HNO$_3$/HF/H$_2$O in a ratio of 3:1:6 at 60–70 °C for 30 min and washed with distilled water and dried in N$_2$ atmosphere. The chemical polishing was chosen as the electrolytic polishing proved to lead to non-homogeneous films [22]. The anodization cell is a two-electrode system consisting of a graphite counter electrode and the titanium metal piece as working electrode, electrolyte of 1 M H$_2$SO$_4$ with 0, 0.25 and 0.5% HF solution contained in a glass chamber and an extended range DC power supply system. The chemically polished titanium metal piece was mounted as anode and graphite serves as cathode. Then they were immersed in the glass chamber containing electrolyte maintained at 1 °C and subjected to anodization by applying constant potential of 40 V for a desired time. Care was taken to maintain constant temperature and velocity of stirring of electrolyte during the anodization. After the completion of anodization, the titanium metal piece was taken out and washed with distilled water and dried in N$_2$ atmosphere. The electrodeposition of cobalt over the obtained anodic titanium oxide (ATO) template was carried out with an aqueous solution of CoSO$_4$·7H$_2$O (240 g/l) and boric acid (40 g/l) for comparison purposes.

2.2. Characterisation of ATO

The anodized titanium oxide was analysed by X-ray diffraction on X'Pert PRO-XRD X-ray diffractometer using CuKα radiation (λ=0.1541 nm) in the range of 10–60°. Also, the surface morphology of the porous titanium film was analysed by field-enhanced scanning electron microscopy (FE-SEM) in LEO 1530 FE-SEM instrument.

2.3. Growth and characterisation of CNTs

The CNTs were grown over an ATO template by CVD method. The ATO template is taken in a ceramic boat and kept in a quartz tube and heated to 650 °C in Ar atmosphere. The carbon source acetylene gas (30 sccm) is mixed with Ar (100 sccm) and passed into the quartz tube at 650 °C for 2 h. Then the acetylene gas is turned off and Ar gas flow is continued for another 15 h at 600 °C (annealing). After 15 h, the system is cooled to room temperature with Ar flow. Then the sample is taken out from the boat and treated with 23% HF for 30 h, filtered and washed in order to remove the ATO template. The morphology of the CNTs grown over the ATO template was analysed by SEM analysis. The CNTs grown over the ATO
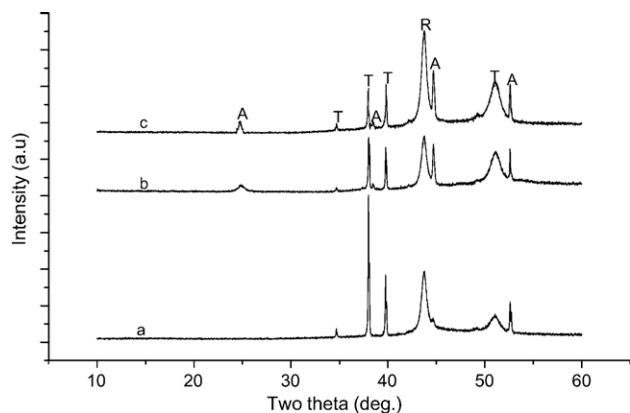
Fig. 1. XRD patterns of titanium oxide anodized in different conditions; (a) in 1 M H_2SO_4; (b) in 1 M H_2SO_4 + 0.25% HF; (c) in 1 M H_2SO_4 + 0.5% HF for 72 h at 40 V (T—Titanium, A—Anatase, R—Rutile).

template, as they were, were cleaned with ethanol and subjected to SEM analysis in Hitachi SEM instrument operating at 50 kV. The features of the CNTs were studied by transmission electron microscope (TEM) using Hitachi H-800 instrument at an accelerating voltage of 150 kV. In order to get more insights about the wall structure of CNTs, high-resolution TEM (HRTEM) images were also obtained on Philips TECNAI F-30 FEG instrument at an accelerating voltage of 300 kV. For both TEM and HRTEM, the CNT sample was dispersed in dry ethanol with an ultra-sonic machine and then deposited on a copper grid with a holey carbon film. Using X'Pert PRO-XRD instrument with CuKα radiation (λ=0.1541 nm), the XRD pattern of the purified CNT sample was recorded in the range 20–50° with a scan rate of 0.050640°/s. Further, the vibrational characteristics of CNTs were recorded with Raman spectroscopy (Renishaw) in the range 1000–2000 cm^{-1}.

3. Results and discussion

3.1. XRD and SEM analyses of anodized titanium oxide

The anodization of Ti was carried out with varying HF concentrations in order to get well ordered porous TiO_2. The XRD patterns of the anodized TiO_2 in 1 M H_2SO_4 with different amounts (0, 0.25 and 0.5%) of HF at 40 V for 72 h are presented in Fig. 1. It claims the presence of both anatase and rutile phases of TiO_2 [27,28]. It is observed that peaks corresponding to Ti are dominating than peaks for titanium oxide (Fig. 1a), indicating that anodization in 1 M H_2SO_4 does not lead to the formation of more titanium oxide. When 0.25% HF is introduced in the electrolyte system, the intensity of the peaks (Fig. 1b) corresponding to the anatase and rutile phase increases significantly. Further, additional peaks for anatase phase are
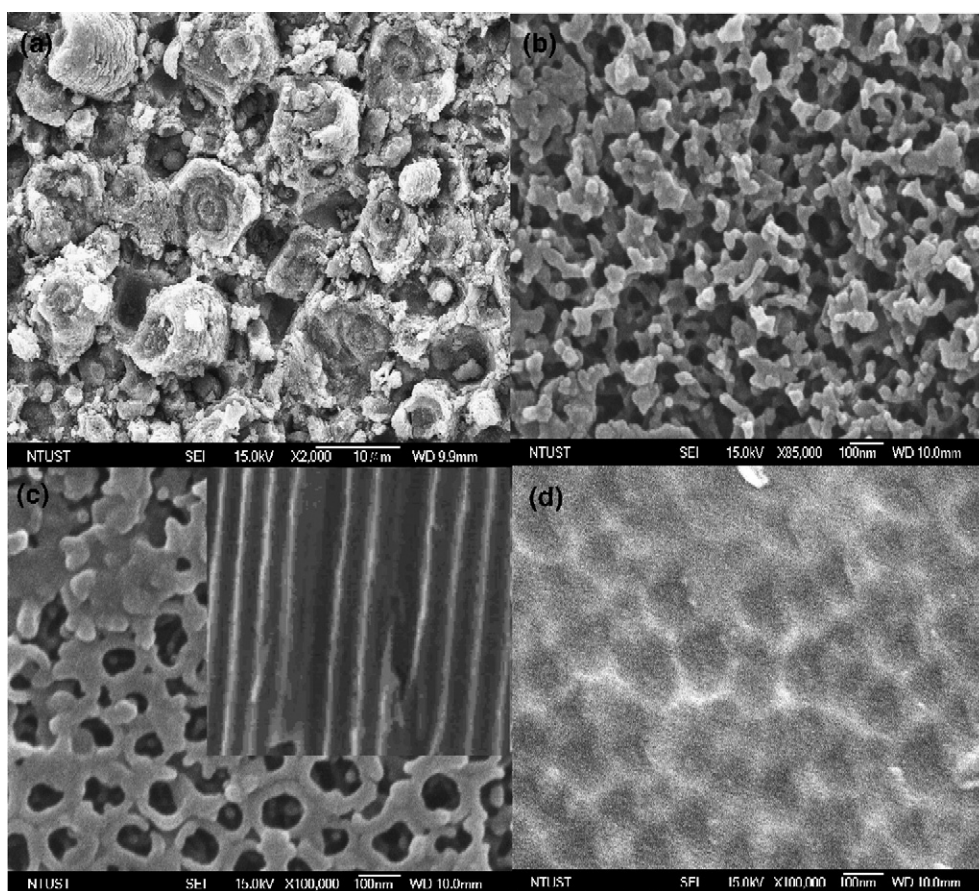

Fig. 2. SEM images of titanium oxide anodized in different conditions; (a) in 1 M H_2SO_4; (b) in 1 M H_2SO_4 + 0.25% HF; (c) in 1 M H_2SO_4 + 0.5% HF for 72 h and (d) in 1 M H_2SO_4 + 0.5% HF for 5 h, at 40 V.
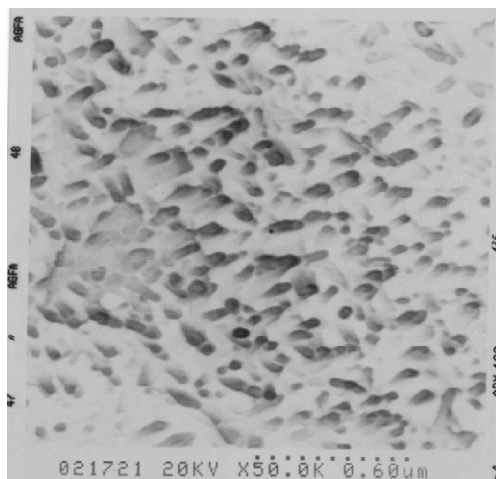
Fig. 3. SEM image of CNTs grown over ATO template before purification.

emerging. When the HF concentration is increased to 0.5% at 40 V for 72 h, the intensity of the peaks for anatase and rutile phases is increased in a greater extent. Generally, XRD patterns show that when increasing the HF concentration in electrolyte under constant potential and anodization time, the anatase and rutile phases appear gradually. Further, it is observed that when increasing the HF concentration from 0 to 0.5%, the intensity of the peaks of titanium on the XRD pattern is found to decrease significantly. The increase in peak intensity for TiO_2 with a fall in intensity of Ti peaks with increasing HF concentration indicates that the formation of TiO_2 with anatase and rutile phases increases with increasing HF concentration.

The morphology of the titanium surface anodized at different experimental conditions was analysed by SEM and the representative images are presented in Fig. 2a–d. It is observed from Fig. 2a, that the titanium surface anodized only in 1 M H_2SO_4 for 72 h shows a rough surface without any regular pore formation indicating that anodization in 1 M H_2SO_4 at 40 V for 72 h does not lead to the formation of ordered pores, even though TiO_2 is formed on the surface as revealed by the XRD analysis. When 0.25% of HF was introduced in the electrolyte and

anodized for 72 h, a sponge like structure (Fig. 2b) was observed without the appearance of uniform pores. Clear pores with a definite size are not seen on the surface. But structured pores with size of 70–80 nm were observed on the surface (Fig. 2c) of titanium metal anodized for 72 h in 1 M H_2SO_4 + 0.5% HF electrolyte solution at 40 V. The cross-sectional view of ATO template presented as inset in Fig. 2c further confirming the formation of uniform channels, even though the outer surface of the template is not uniform due to anodization in acid medium for long time. The onset of pore formation is shown clearly in Fig. 2d, which is the SEM image of Ti surface anodized for 5 h in 1 M H_2SO_4 + 0.5% HF solution at 40 V. It clearly shows the initiation of pore formation and the pore depth increases with increasing anodization time. Further, all the SEM images reflect that, several hours of continuous pore drilling at the inner interface and oxide dissolution are necessary to obtain uniform pores. The key processes for the formation of pores on Ti metal are (i) the oxide growth at the surface of the metal, (ii) metal ion (Ti^{4+}) migration from the metal at the metal/oxide interface under the applied electric field and (iii) field assisted dissolution of the oxide at the oxide/electrolyte interface [29,30]. When increasing the anodization time, the Ti ions are migrated to the solution, resulting in a significant loss of material and making the outer surface non-uniform. It may be due to the fact that titanium oxide can be etched at a high rate in the presence of HF solution. If the etching rate of the oxide in solution is comparable with that of the field-enhanced dissolution, the titanium oxide either in the wall or at the pore bottom will dissolve at a balanced rate resulting in a constant pore depth [24]. Because of the semiconducting nature of the TiO_2, similar behaviors as those of alumina are not observed. Based on XRD and SEM analyses of anodized TiO_2, the anodization for 72 h in 1 M H_2SO_4 + 0.5% HF at a constant applied potential of 40 V was used for further experimental studies.

3.2. SEM and TEM analyses of CNTs

In order to study the morphology of as-grown CNTs before purification, SEM analysis was carried out and a typical image
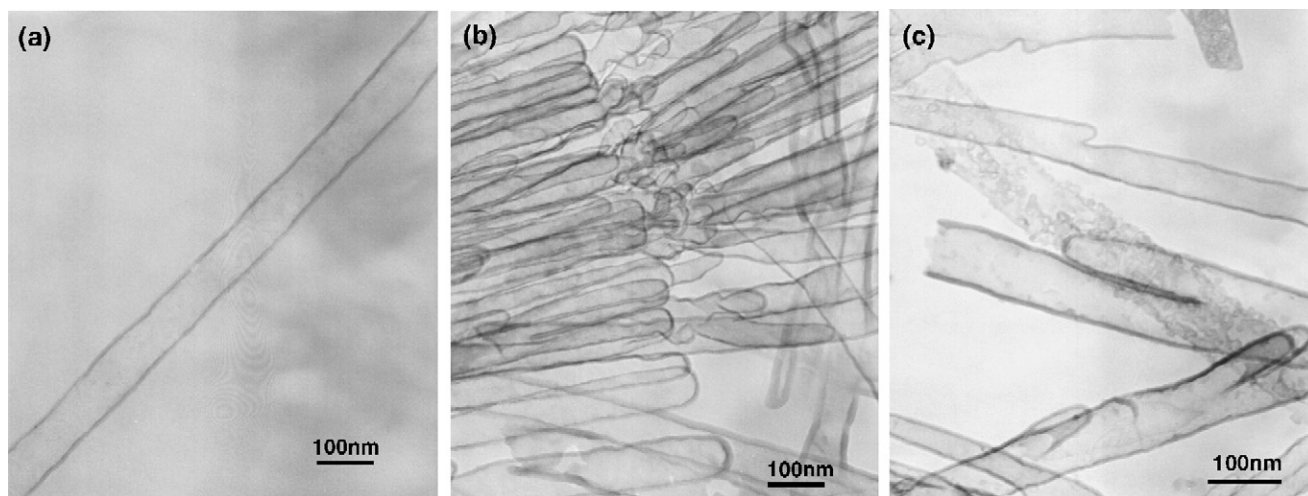

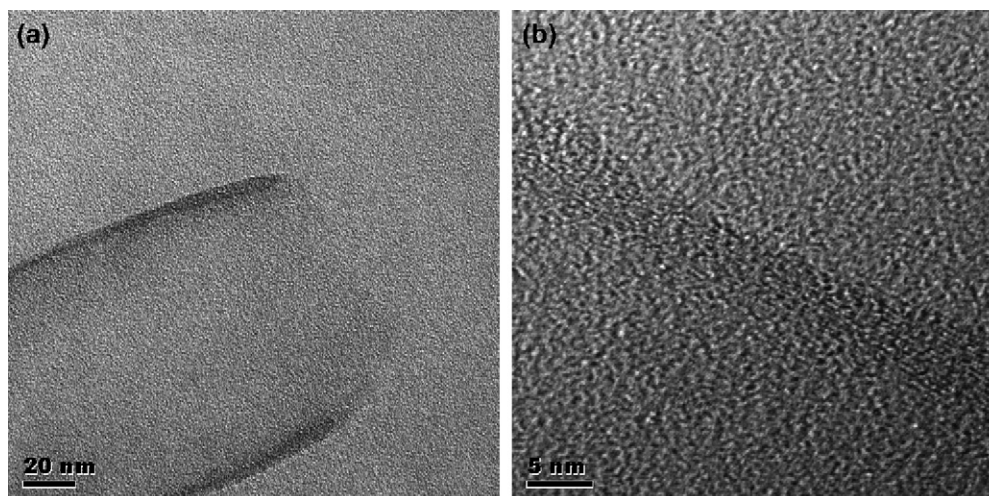Fig. 4. TEM images of CNTs formed over ATO template.

Fig. 5. HRTEM images of CNTs grown over ATO template.

is given in Fig. 3. It can be seen that the CNTs are grown from the pores of ATO and are confined inside the pores of the template. Most of the CNTs slightly overgrew out of the pores of the template. Also, the density of the grown CNTs is found to be higher, which reflects the pore density of ATO. The morphology of purified CNTs is analysed by TEM and the images are presented in Fig. 4. It is clearly seen that CNTs with diameter of 70–80 nm were observed. The thickness of the walls of the CNTs is found to be homogeneous. Also, the length of the formed CNTs is in the range of several micrometers with wide inner space. Further, most of the CNTs are found to be straight with very few of them having branches. In Fig. 4b, the closed end structure of the CNTs indicates that the CNTs are formed from the bottom of the pores (barrier layer). The open end structure is clearly noticed in Fig. 4c. The wall thickness is found to be very thin and uniform. Since, CNTs are used to copy

the internal pore structure of the template, their morphological study gives a reliable approach to study the pore structure of ATO. The branched structure shown by the CNTs reflects the three-dimensional internal pore structure of the ATO template. Further, the walls of the CNTs are smooth with homogeneous thickness indicating the uniformity of the internal surface of pores. The domelike structure (closed end structure in Fig. 4b) of the bottom of CNTs is reflecting the structure of the so-called barrier layer, a thin oxidized layer separating the porous layer from the Ti metal substrate. This type of porous layer is commonly observed in porous alumina. When the CVD process is carried out at 650 °C, the decomposition of acetylene in the pores results in carbon deposition on the internal pore surface, which constitutes the tubes and copies the three-dimensional channel structure of the template. The formation of CNTs inside the ATO pores without any metal catalyst is a strong indication
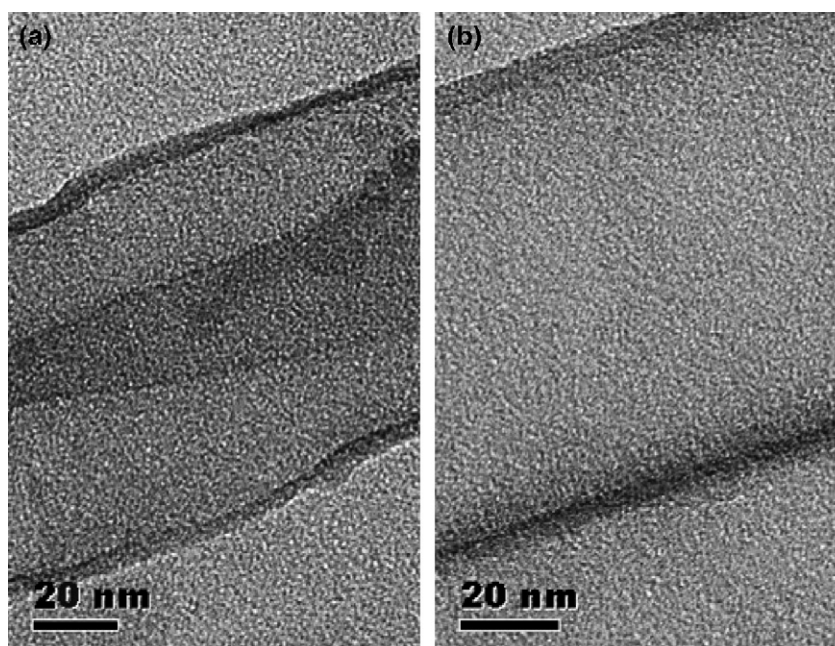

Fig. 6. HRTEM images showing the wall structure of CNTs grown with different deposition times; (a) 4 h and (b) 5 h.
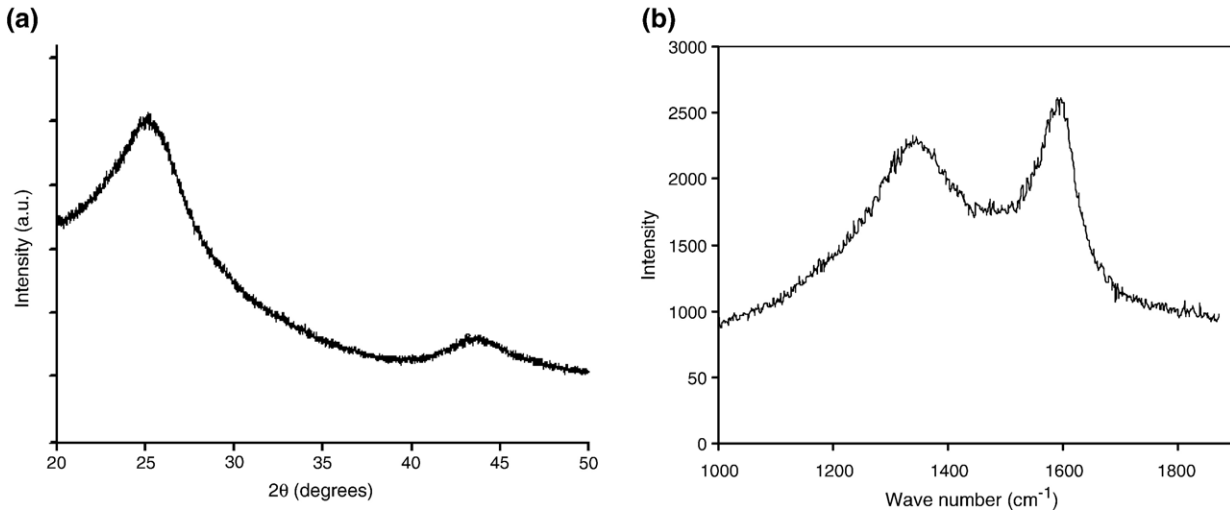
Fig. 7. XRD (a) and Raman spectrum (b) of CNTs grown over ATO template.

of the catalytic behavior of the internal pore surface of TiO_2, in addition to template function. Hence, it is assumed that the Lewis acid sites of the TiO_2 are responsible for their catalytic activity. Since, anatase and rutile forms of TiO_2 are widely used as catalyst, catalyst support and photocatalyst in many chemical transformations, it is expected that the strength of Lewis acid sites of porous TiO_2 is high enough to catalyse the decomposition of acetylene at 650 °C. From the morphology of CNTs, it is assumed that the internal surface of pores is uniform and hence uniform catalytic activity is expected. Therefore, the chance for the decomposition of acetylene is the same at any point of the walls and hence the surface is uniformly covered by carbon deposits during the CVD process, leading to the formation of carbon nanotube-like structure.

3.3. Tube wall structure from HRTEM analysis

HRTEM measurements were also carried out to study the wall structure of the formed CNTs. Fig. 5a–b shows the HRTEM images of CNTs formed over the ATO template without Co metal catalyst. It is observed that the tubes have a relatively larger diameter and are found to be multi-walled. The wall thickness at the middle is in the range 2–3 nm (Fig. 5b) and the walls are found to have good crystallinity. The open end structure of the tips is also clearly noticed in Fig. 5a. Because of the amorphous background due to the specimen support film, the number of graphene layers is not clear. But, it can be guessed that the wall consists of around 5 graphene layers. It indicates that the CNTs are made of typical turbostratic graphite [31,32]. It is interesting to note that the internal diameter of the CNTs is around 70 nm, which is different from that of CNTs grown over AAO [18], which is around 10 nm. This is due to the fact that only a lesser number of graphene layers constitute the walls of CNTs, as shown by HRTEM. The CNTs are formed on the inner surface of the pores of the ATO template due to the catalytic decomposition of acetylene on Lewis acid sites of TiO_2. The Lewis acid sites in the pores could act as a catalyst in forming few walls of the CNTs. But, after few walls are formed on the inner surface, the Lewis acid sites of ATO exist underneath the carbon nanotube walls. Due to this phenomenon, the Lewis acid sites of TiO_2 can not act as a catalyst anymore and the catalytic decomposition of acetylene stops, typically resulting in a very thin wall as opposed to CNTs made by other methods. In order to confirm the same, CNTs were grown with
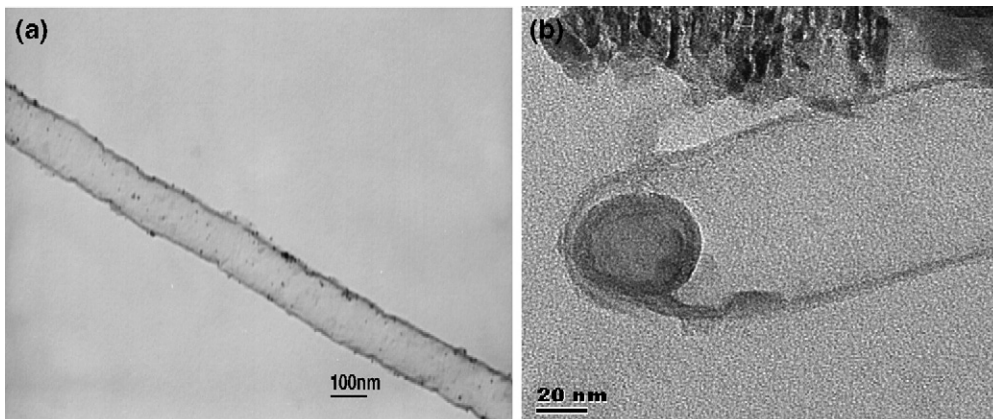

Fig. 8. TEM (a) and HRTEM (b) images of CNTs formed over anodized titanium oxide template with Co catalyst.

deposition time of 4 and 5 h under similar experimental conditions and the corresponding HRTEM images are presented in Fig. 6a and b, respectively. The wall thickness of CNTs in both cases is around 2–3 nm. When comparing with that of CNTs with deposition time of 2 h (Fig. 5a), no significant increase in wall thickness is observed. It indicates that wall thickness of CNT is independent of carbon deposition time, which is opposite to the observation made by Kyotani et al. [18] over AAO template. The wall thickness is not increased by an increase in carbon deposition time indicating that the decomposition of acetylene, leading to formation of CNTs, is due to the Lewis acid sites of TiO_2 and not due to the thermal decomposition.

3.4. XRD and Raman spectroscopy of CNTs

The structure and nature of the CNTs were analysed by X-ray diffraction and Raman spectroscopy and are presented in Fig. 7a and b, respectively. In XRD, two major peaks are observed, one is near $2\theta = 26°$ corresponding to the 002 reflection, that related to the stacking order in polyaromatic solids. The other small asymmetric peak near 43.5° is due to the 10 reflection of turbostratic carbon. The Raman spectrum shows two strong bands at 1347 and 1592 cm^{-1} confirming the multi-walled nature of the CNTs. These bands correspond to fundamental vibration modes of D_{6h}^4 of graphite [33]. The band at 1592 cm^{-1} (G band) corresponds to the Raman allowed optical mode E_{2g} of two-dimensional graphite, i.e. Raman active in-plane vibrational mode for an infinite or finite hexagonal network. The band at 1347 cm^{-1} (D band) is mainly derived from disordered carbon defects of the MWNTs, and is one of the in-plane vibrational modes. As compared to the G band at 1580 cm^{-1} for the graphitic carbons, the shift in G band towards a higher wavenumber (1592 cm^{-1}) and the I_D/I_G value (0.88) suggest a turbostratic structure, consistent with HRTEM and XRD investigations.

For comparison purposes, CNTs were grown over Co electrodeposited ATO template following the same experimental conditions. The morphology of the formed CNTs after purification was analysed by TEM and HRTEM and the typical images are presented in Fig. 8a and b, respectively. When comparing the morphology as well as wall thickness of the CNTs formed over ATO with and without Co metal catalyst, no significant difference is observed. A metal particle inside the CNTs is clearly observed (Fig. 8b). But, still further detailed study is necessary to study the structural differences between the CNTs formed over the ATO template with and without Co catalyst.

4. Conclusions

Anodized titanium oxide with structured pores was obtained by an anodization process in 1 M H_2SO_4 + 0.5% HF at a constant potential of 40 V for 72 h. Well ordered carbon nanotubes were formed over anodic titanium oxide template by CVD method using acetylene as carbon source. The CNTs are found to have good crystallinity with diameter of 70–80 nm,

similar to that of pores of the template. The formation of CNTs over ATO without metal catalyst indicates that the Lewis acid sites of TiO_2 are having strong enough catalytic activity to decompose the acetylene, leading to the formation of CNTs. The TEM and HRTEM studies indicated that the CNTs are straight, hollow and multi-walled and the wall thickness is around 2–3 nm. The Lewis acid sites of TiO_2 present in the internal surface of the pores play an important role in the catalytic decomposition of acetylene and the formation of CNTs. When increasing the carbon deposition time, the wall thickness of CNTs is not increased, indicating that the decomposition of acetylene is due to the Lewis acid sites of TiO_2 and not due to thermal decomposition. Further, the XRD pattern confirms the turbostratic structure as well as good crystallinity of the CNTs. The Raman spectroscopy confirms the multi-walled nature of CNTs. There is no significant difference in morphology as well as wall thickness observed between the CNTs grown over ATO with and without cobalt catalyst. All the experimental results indicate that the ATO can be used as a template to grow well ordered high quality CNTs with a larger diameter. The selective formation of CNTs over porous titanium surface could be used for the fabrication of nanofunctional devices and the larger size of the CNTs favors higher metal dispersion as well as the accessibility of reactant molecules to metal particles inside the CNTs, when it is used as a catalyst support in various chemical reactions.

References

[1] S. Fan, M.G. Chapline, N.R. Franklin, T.W. Tombler, A.M. Cassel, H. Dai, Science 283 (1999) 512.
[2] A.C. Dillon, K.M. Jones, T.A. Bekkedhal, C.H. Kiang, D.S. Bethune, M.J. Heben, Nature 386 (1997) 377.
[3] J.H. Hafner, C.L. Cheung, T.H. Oosterkamp, C.M. Lieber, J. Phys. Chem., B 105 (4) (2001) 743.
[4] L.P. Biro, S. Lazarescu, P. Lambin, P.A. Thiry, A. Fonseca, B. Nagy, J.B. Nagy, A.A. Lucas, Phys. Rev., B 56 (1997) 12490.
[5] S.J. Tans, A.R.M. Verschueren, C. Dekker, Nature 393 (1998) 49.
[6] R. Martel, T. Schmidt, H.R. Shea, T. Hertel, Ph. Avouris, Appl. Phys. Lett. 73 (1998) 2447.
[7] J.T. Hu, O.Y. Min, P.D. Yang, C.M. Lieber, Nature 399 (1999) 48.
[8] D.-J. Guo, H.-L. Li, J. Electroanal. Chem. 573 (2004) 197.
[9] S. Iijima, Nature 354 (1991) 56.
[10] B.J. Hinds, N. Chopra, T. Rantell, R. Andrews, V. Gavalas, L.G. Bachas, Science 303 (2004) 62.
[11] T. Ebbesen, P.M. Ajayan, Nature 358 (1992) 220.
[12] C. Journet, W.K. Maser, P. Bernier, A. Loiseau, M. Lamy de la Chapelle, S. Lefrant, P. Deniard, R. Leek, J.E. Fischer, Nature 388 (1997) 756.
[13] T. Guo, P. Nikolaev, A. Thess, D.T. Colbert, R.E. Smalley, Chem. Phys. Lett. 243 (1995) 49.
[14] M.J. Yacaman, M.M. Yoshida, L. Rendon, J.G. Santiesteban, Appl. Phys. Lett. 62 (1993) 202.
[15] J. Li, C. Papadopoulos, J.M. Xu, Appl. Phys. Lett. 75 (1999) 367.
[16] J.S. Suh, J.S. Lee, Appl. Phys. Lett. 75 (1999) 2047.
[17] G. Che, B.B. Lakshmi, C.R. Martin, E.R. Fisher, Chem. Mater. 10 (1998) 260.

[18] T. Kyotani, L.F. Tsai, A. Tomita, Chem. Mater. 8 (1996) 2109.
[19] L. Jing, M. Martin, H.L. Tom, Chem. Mater. 10 (1998) 1963.
[20] R. Asahi, T. Morikawa, T. Ohwaki, K. Aoki, Y. Taga, Science 293 (2001) 269.
[21] T. Albrektsson, P.I. Branemark, H.A. Hansson, J. Lindstrom, Acta Orthop. Scand. 52 (1981) 155.
[22] V. Zwilling, M. Aucouturier, E. Darque-Ceretti, Electrochim. Acta 45 (1999) 921.
[23] V. Zwilling, E. Darque-Ceretti, A. Boutry-Forveille, D. David, M.Y. Perrin, M. Aucouturier, Surf. Interface Anal. 27 (1999) 629.
[24] D. Gong, C.A. Grimes, O.K. Varghese, W. Hu, R.S. Singh, Z. Chen, E.C. Dickey, J. Mater. Res. 16 (12) (2001) 3331.
[25] R. Beranek, H. Hildebrand, P. Schmuki, Electrochem. Solid-State Lett. 6 (3) (2003) B12.
[26] J. Choi, R.B. Wehrspohn, J. Lee, U. Gosele, Electrochim. Acta 49 (2004) 2645.
[27] J.-H. Park, Y.-K. Lee, K.-M. Kim, K.-N. Kin, Surf. Coat. Technol. 195 (2–3) (2005) 252.
[28] B. Yang, M. Uchida, H.-M. Kim, X. Zhang, T. Kokubo, Biomaterials 25 (2004) 1003.
[29] V.P. Parkhutik, V.I. Shershulsky, J. Phys. D: Appl. Phys. 25 (1992) 1258.
[30] D.D. Macdonald, J. Electrochem. Soc. 140 (1993) L27.
[31] V. Ivanov, J.B. Nagy, P. Lambin, A.A. Lucas, X.B. Zhang, X.F. Zhang, D. Bernaerts, G. Vantendeloo, S. Amelinckx, J. Vanlanduyt, Chem. Phys. Lett. 223 (1994) 329.
[32] K. Hernadi, A. Fonseca, J.B. Nagy, D. Bernaerts, A.A. Lucay, Carbon 34 (1996) 1249.
[33] P.S. Eklund, J.M. Holden, R.A. Jishi, Carbon 33 (1995) 959.